Supporting Information

Room temperature continuous flow synthesis of γ-valerolactone and N-containing heterocycles over a Ru supported on a bimodal N, S-doped cubic mesoporous carbon

Hamzeh H. Veisi,[a, b] Babak Karimi,*[a, c] Mohsen Heydari,[a] Rafael Luque[b, d]*

a Department of Chemistry, Institute for Advanced Studies in Basic Sciences (IASBS), PO. Box 45195-1159, Prof. Sobouti Boulevard, Zanjan 45137-66731, Iran.
b Departamento de Química Orgánica, Universidad de Córdoba, Edificio Marie Curie (C-3), Ctra Nnal IV-A, Km 396, E-14014 Córdoba, Spain.
c Research Center for Basic Sciences & Modern Technologies (RBST), Institute for Advanced Studies in Basic Sciences (IASBS), Prof. Sobouti Boulevard, Zanjan 45137-66731, Iran.
d Universidad ECOTEC, Km. 13.5 Samborondón, Samborondón, EC092302, Ecuador.

*Corresponding authors: E-mail: rafael.luque@uco.es; karimi@iasbs.ac.ir.

Table of Contents

Figures

General procedure for the continuous conversion of levulinic acid into gamma valerolactone reactions

Flow reactions were conducted using an H-Cube instrument from Thalesnano Inc. equipped with a back-pressure regulator. Various concentrations of LA or methyl levulinates (0.1 to 3 M) were passed at a flow rate of 0.1 mL.min^{-1} through a fixed bed at different temperatures (30-90 °C) containing 0.1 g catalyst under different hydrogen pressure (10-60 bar). The identity of the products was confirmed by GC-MS. Response factors of reaction products were determined by GC analysis using standard compounds in calibration mixtures of specified compositions.

The operation of the H-Cube mini plus without hydrogen gas

H-Cube Mini Plus can work in hydrogen mode ON for hydrogenations, or hydrogen mode OFF for catalytic reactions that do not require hydrogen. In the absence of hydrogen gas, the pressure can be produced by liquid phase.

The analysis of reaction mixtures with GC-MS and GC-FID

All products also were identified by GC-MS, a coupled Agilent 7820A GC-5977B/MSD, equipped with a column Agilent 19091S-433UI (HP-5MS Ultra Inert; 30 m× 250 µm×0.25 µm; -60 °C-325 °C). An auto-injector was employed to inject the 1 µl of samples at 250 °C and was set to a 50:1 split ratio. Helium was used as carrier gas with flow rate of 1.8 mL min^{-1}. The temperature program was set as follows: the oven initially started at 50 °C, held for 2 min, raised to 250 °C at a rate of 20 °C.min^{-1}, and held for 10 min at 250 °C. The ion source of the mass spectrometer was set at 280 °C. The peaks were analysed on the basis of retention time and using the NIST database and retention index.

The reaction mixtures were analysed by gas chromatography (GC) using a 6890 N chromatograph system (Agilent) equipped with an HP-5 column (30 m × 0.32 mm × 0.23 mm) using a flame ionization detector (FID) (injector 250 °C, detector 250 °C). The oven initially started at 50 °C, held for 3 min, raised to 250 °C at a rate of 20 °C.min^{-1}, and held for 20 min. Response factors of the reaction products were determined with respect to the original starting materials from GC analysis using known compounds in calibration mixtures of specified compositions.

In addition, some samples were analysed with a Hewlett Packard HP 5890 Series II Gas Chromatograph, provided with an EQUITY^{TM}-1 (60 m × 0.25 mm × 0.25 µm) column and an FID detector (Supelco Analytical, Bellefonte, PA, USA). The temperature in the injector as

well as in the reactor was 250 °C. The oven temperature program used was from an initial temperature of 50 °C for 5 minute that was increased up to 250 °C with a heating rate of 20 °C.min^{-1} and remained constant at that temperature for 10 min.

Calculation of Weight Hourly Space Velocity (WHSV) and space time yield (STY)

Weight Hourly Space Velocity (WHSV) = $\frac{g_{(feed)}}{g_{(cat)}.h}(h^{-1})$

Space-time yield (STY) = $\frac{g_{(Levulinic\ acid)}}{g_{(Ruthenium)}.h}(h^{-1})$

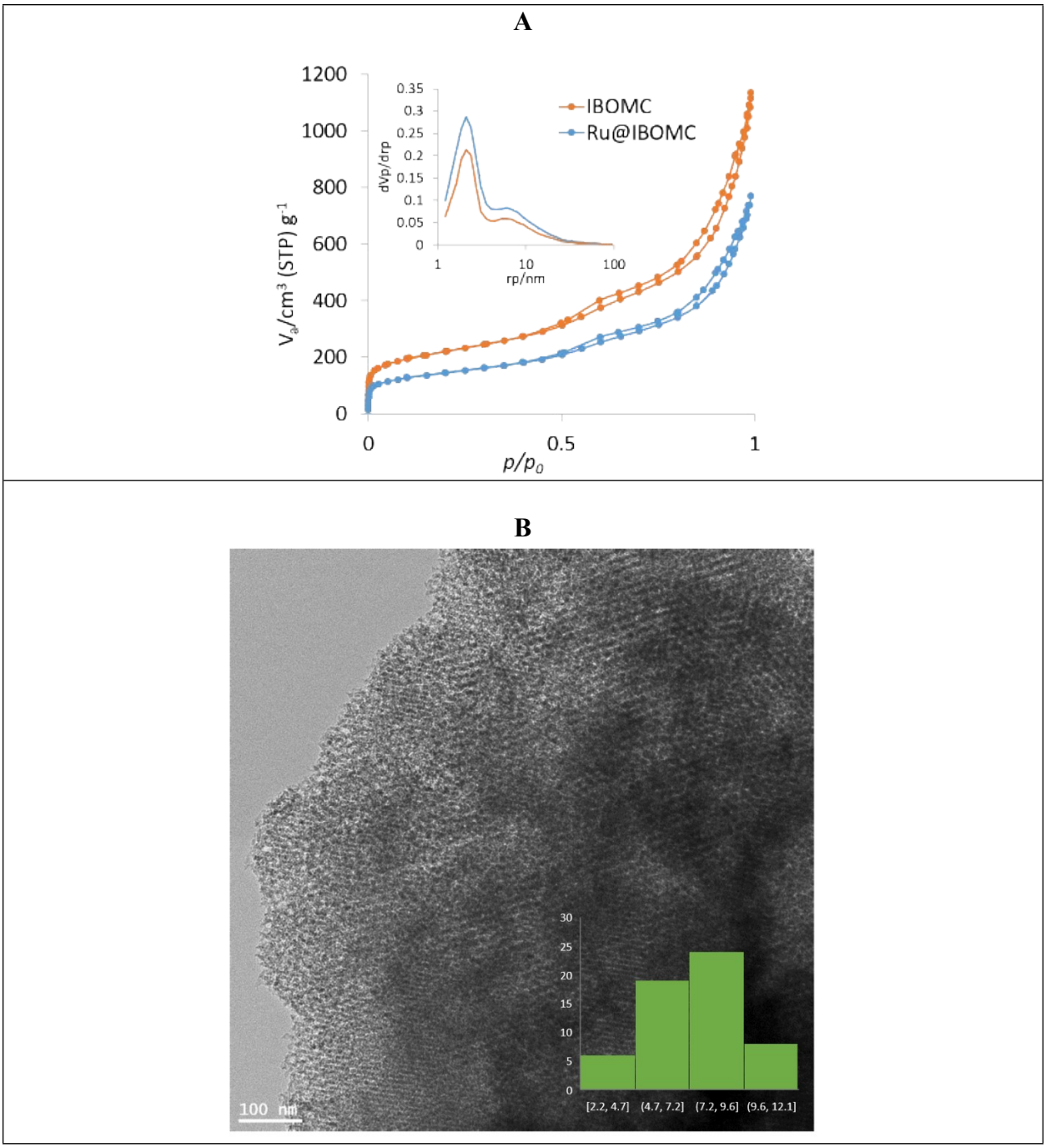

Figure S 1. A) N_2 adsorption-desorption isotherms, and pore size distribution curves (evaluated using the DH method) of the synthesized carbon and catalyst (the orang diagram for IBOMC; the blue diagram for Ru@IBOMC), B) TEM of Ru@IBOMC

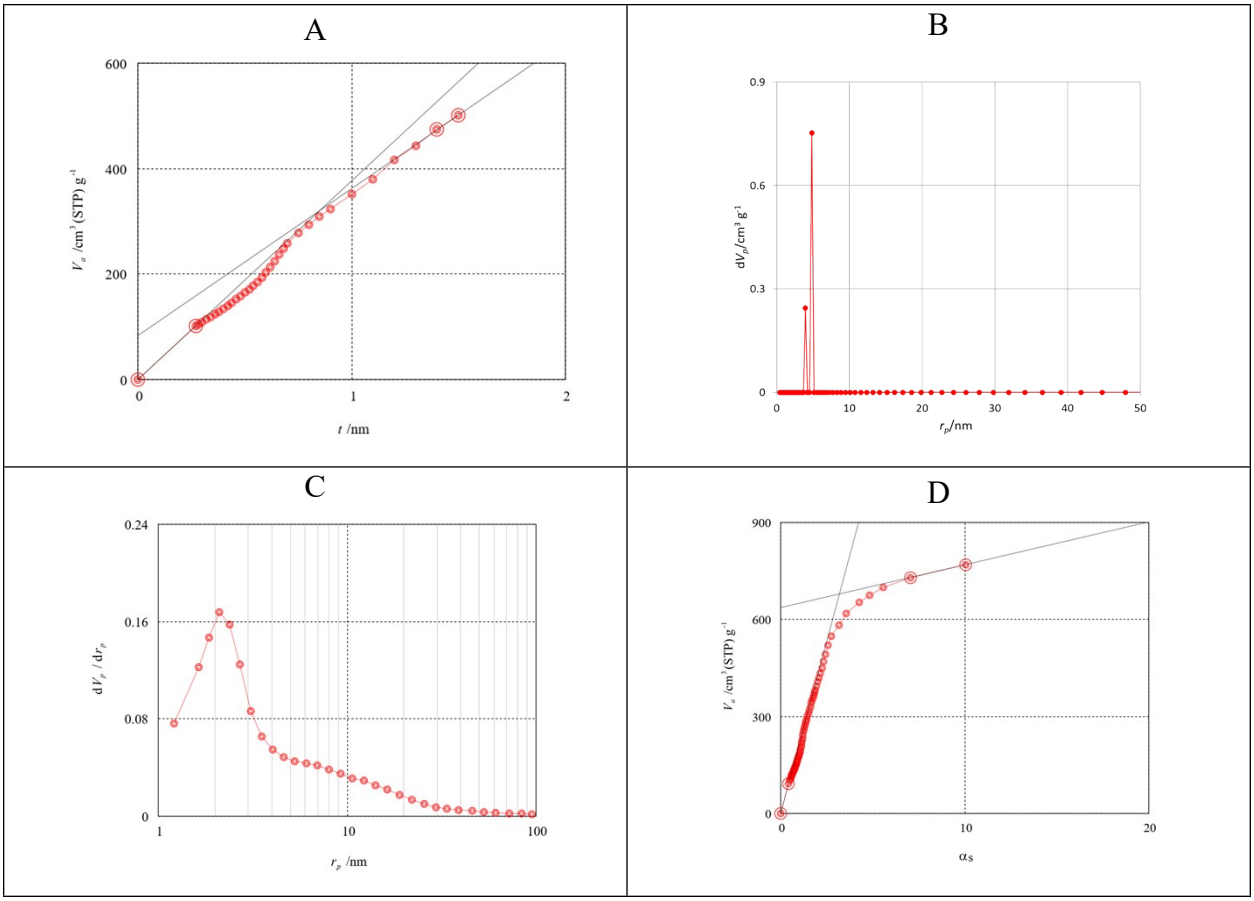

Figure S 2: A) t-plot of Ru@IBOMC, B) NLDFT of Ru@IBOMC with PSD of $r_{p,peak}$ = 3.95 nm and 4.82 nm, C) BJH of the catalyst, D) alpha-plot of the catalyst.

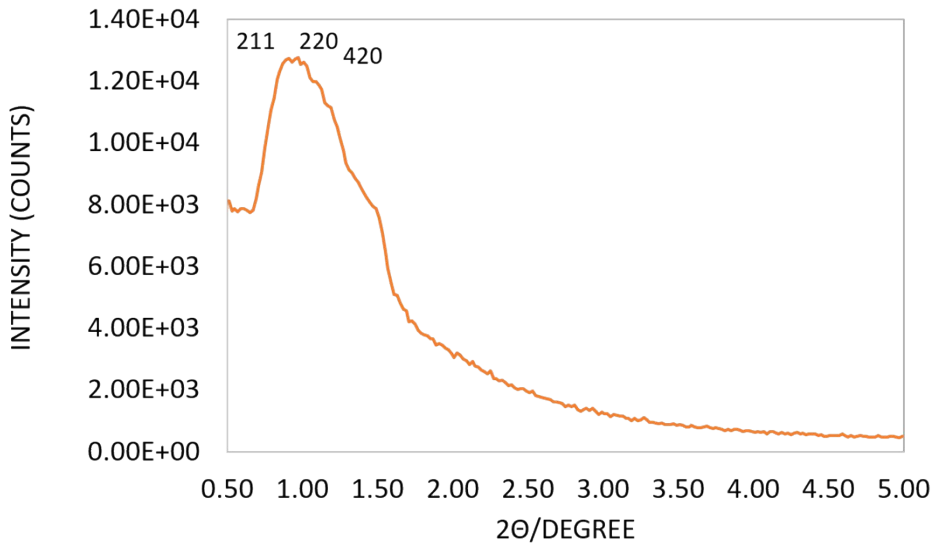

Figure S 3. Low angel XRD of IBOMC

Table S1: Low angel XRD peak list of IBOMC

Pos.[°2Th.]	Height [cts]	d-spacing [Å]	Rel. Int. [%]
0.91 (2)	2893 (548)	97.474	100
1.49 (1)	1387 (129)	59.32681	47.94

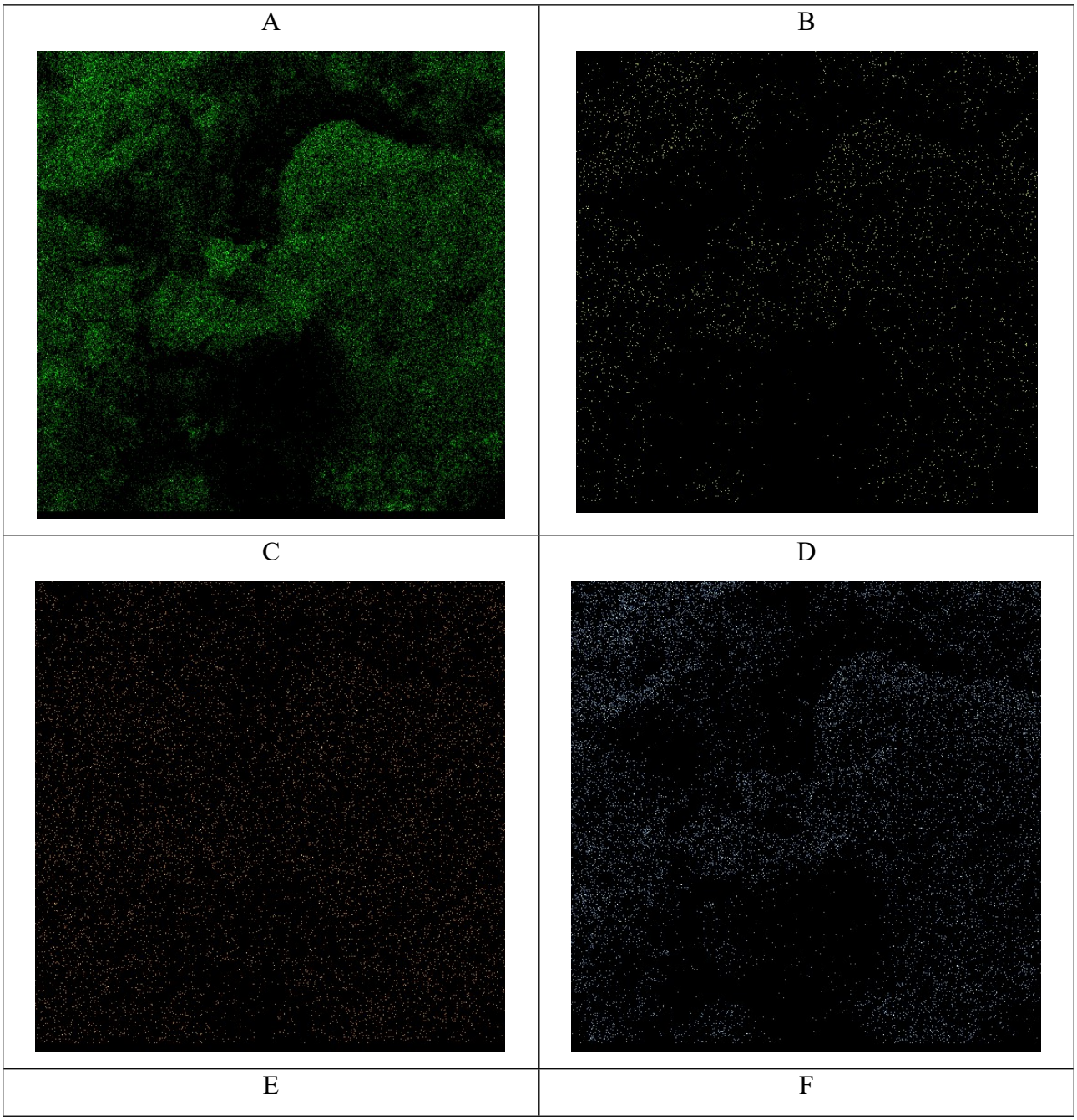
A
B
C
D
E
F

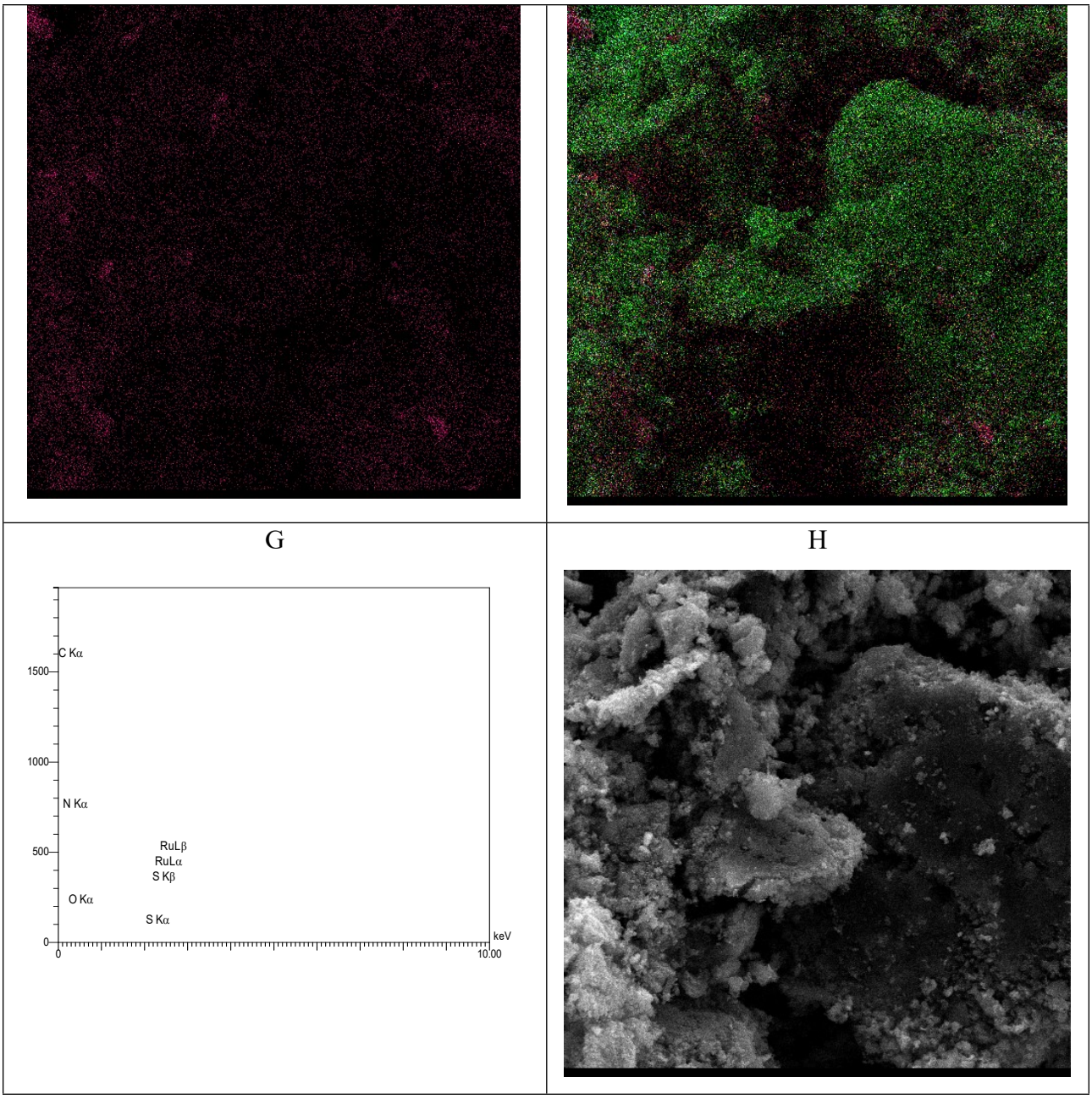

Figure S 4: Elemental mapping images of Ru@IBOMC: Dispersion of Carbon element (A), Nitrogen element (B) Sulfur element (C) Oxygen element (D) Ruthenium element (E), and the combine of all elements (F) on the surface of Ru@IBOMC; EDX analysis of Ru@IBOMC (G); SEM of Ru@IBOMC (H).

Table S 2: Quantitative EDX Results of Ru@IBOMC

Elt	Line	Int	Error	K	Kr	W%	A%	ZAF	Ox%	Pk/Bg	Class	LConf	HConf	Cat#
C	Ka	121.8	2.9137	0.7562	0.5792	63.67	80.69	0.9098	0.00	673.46	A	62.18	65.15	0.00
N	Ka	3.0	2.9619	0.0178	0.0136	7.24	7.87	0.1880	0.00	31.19	A	6.17	8.31	0.00
O	Ka	16.7	3.0100	0.0318	0.0244	8.50	8.09	0.2864	0.00	34.53	A	7.97	9.04	0.00
S	Ka	9.2	1.5207	0.0095	0.0073	0.79	0.37	0.9216	0.00	5.89	A	0.72	0.85	0.00
Ru	La	78.6	2.1247	0.1848	0.1415	19.80	2.98	0.7147	0.00	19.96	A	19.23	20.38	0.00
				1.0000	0.7660	100.00	100.00		0.00					0.00

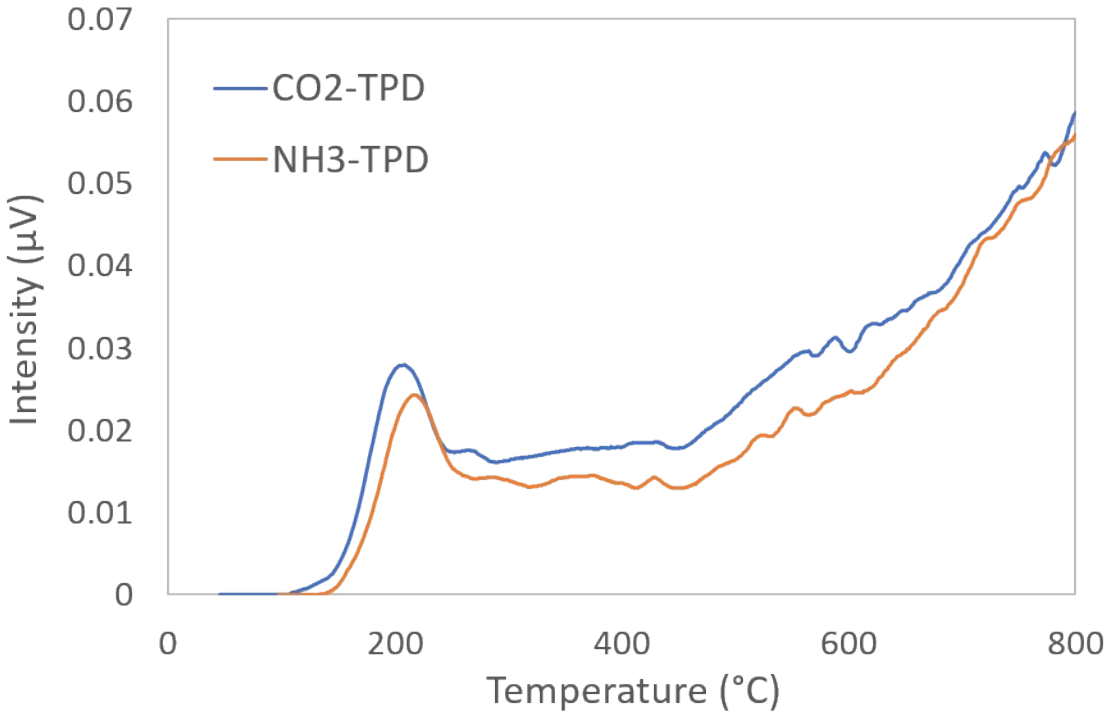

Figure S 5: CO_2 and NH_3 TPDs of IBOMC

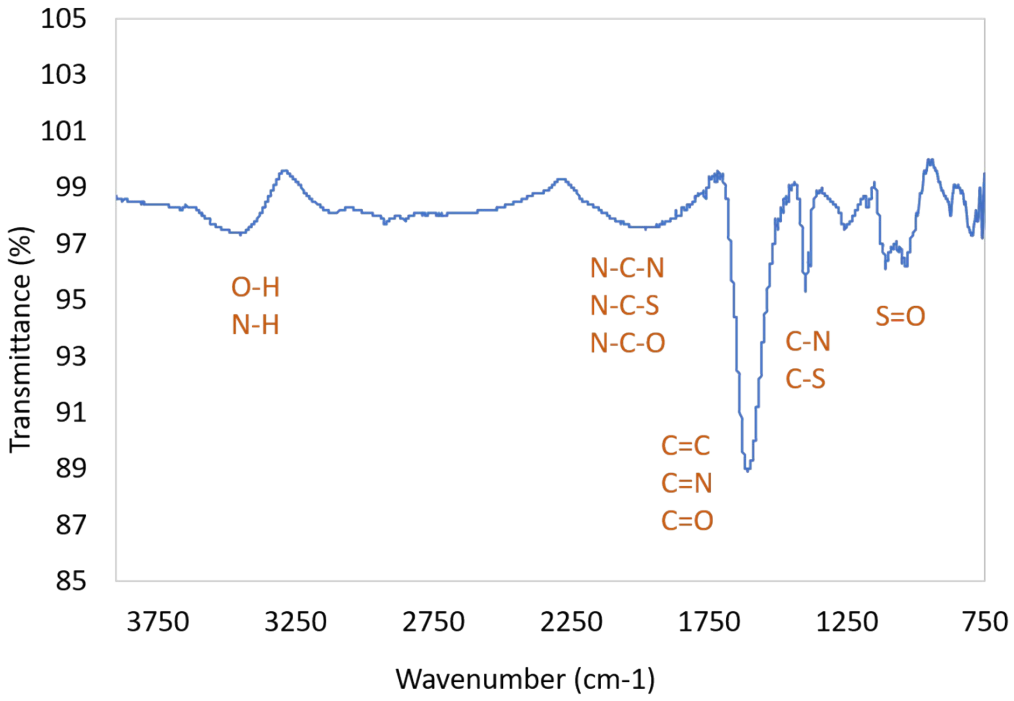

Figure S 6: FT-IR of IBOMC

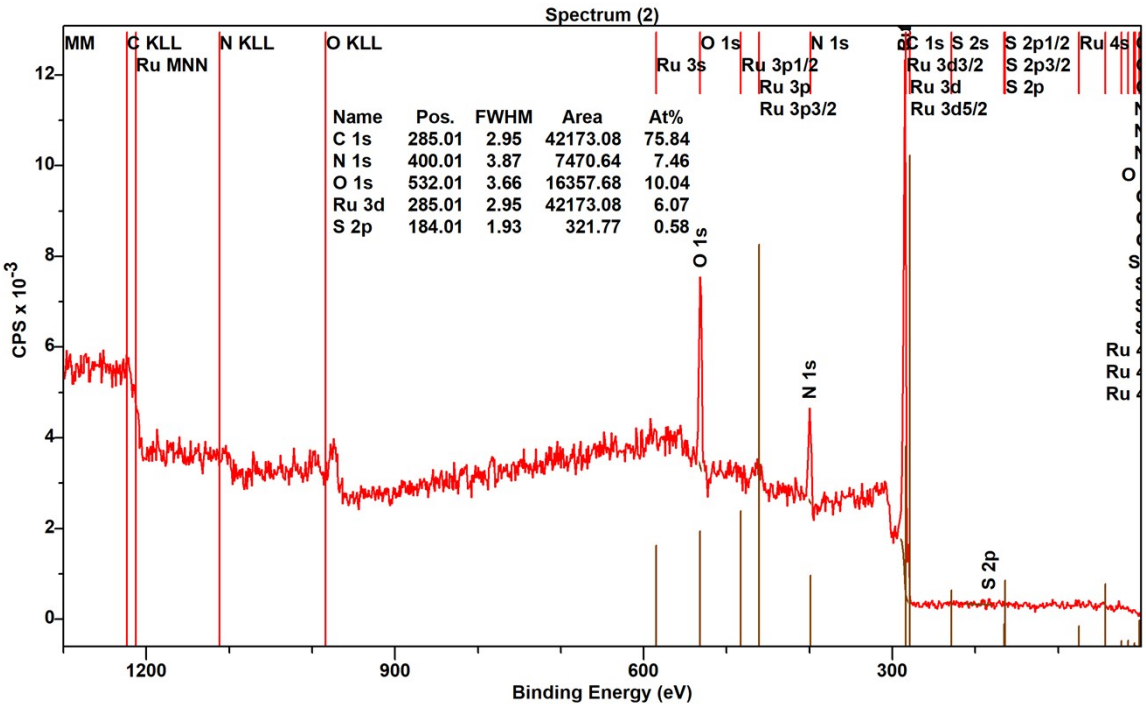

Figure S 7. XPS of Ru@IBOMC

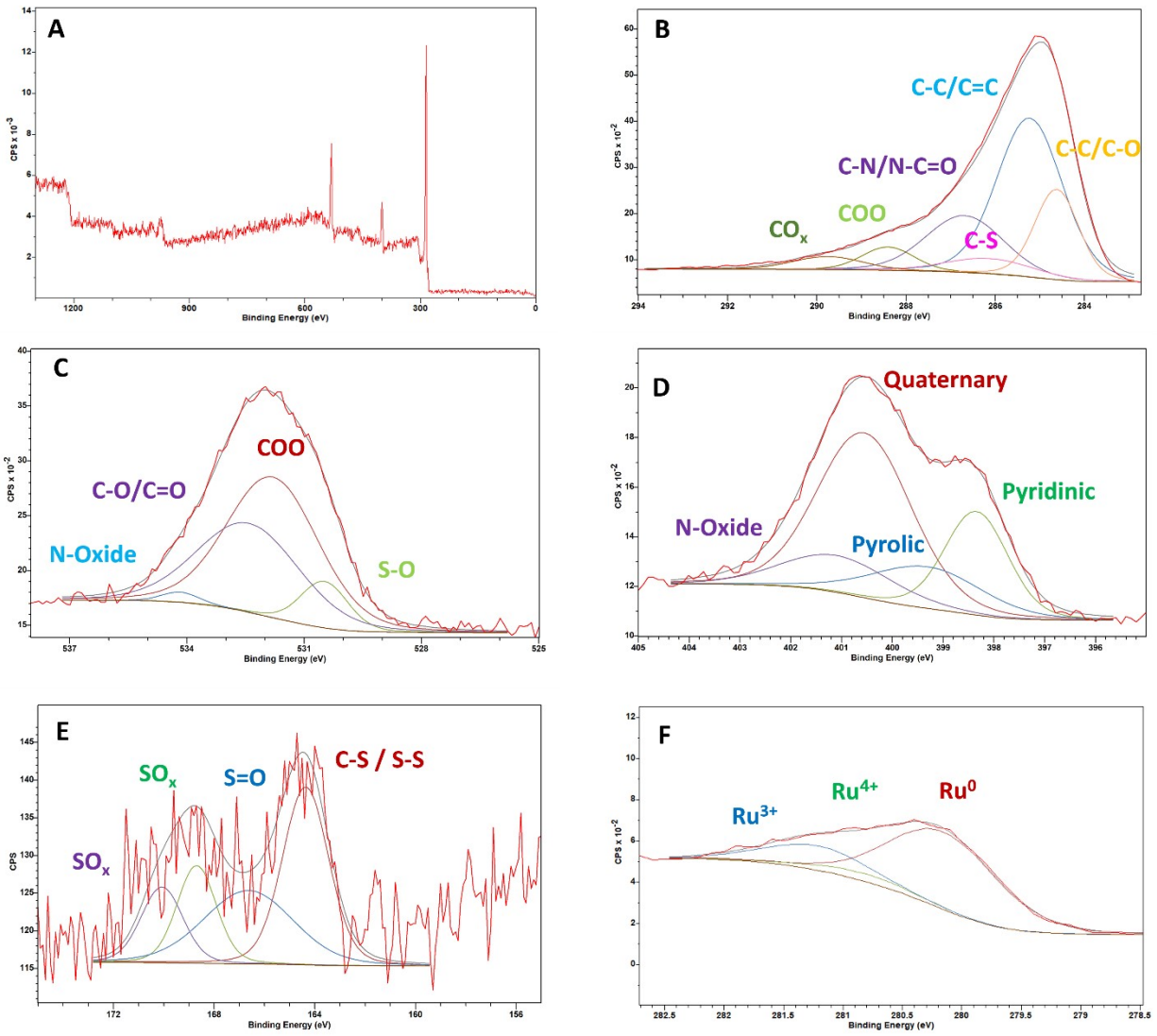

Figure S 8: XPS deconvolution of Ru@IBOMC

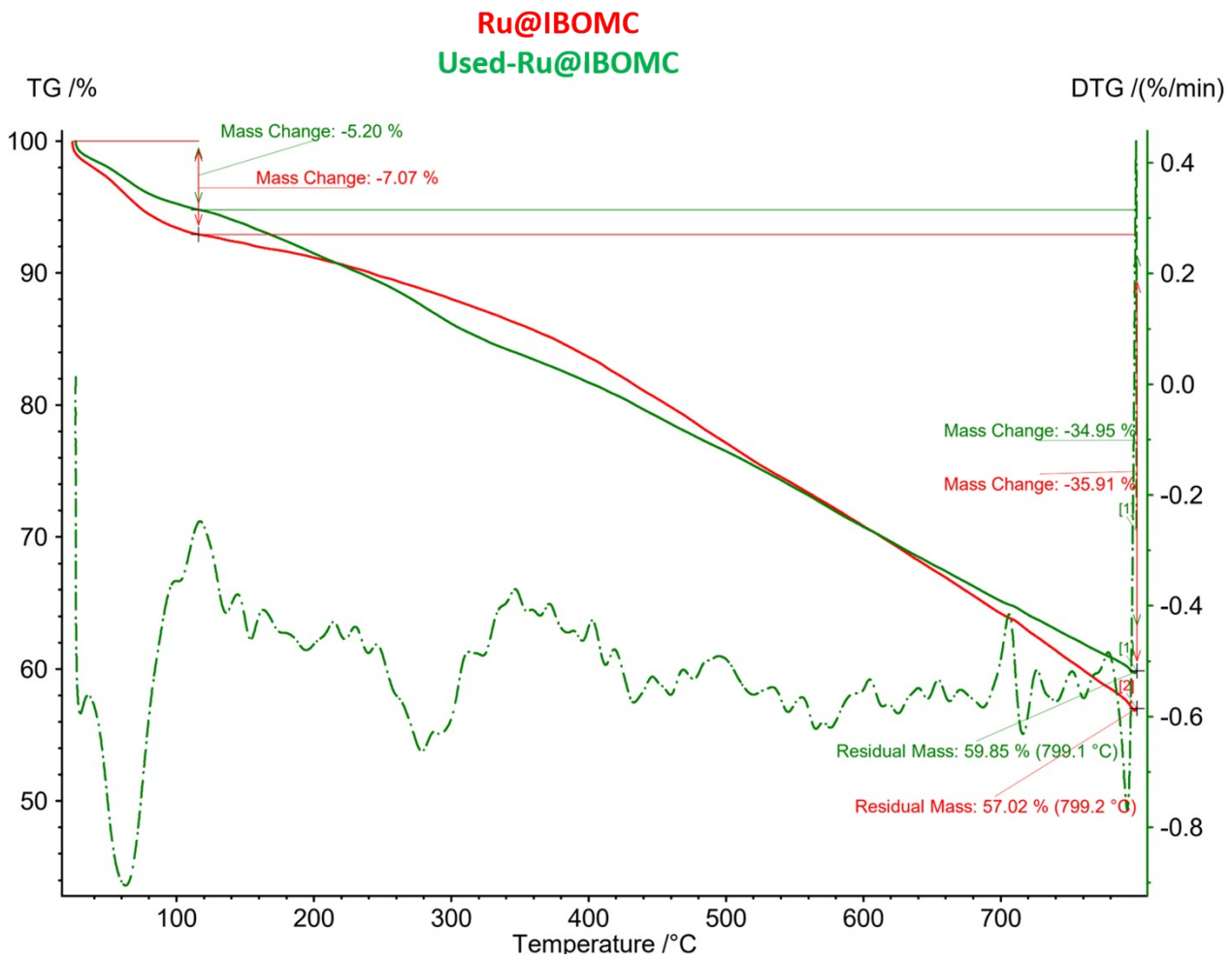

Figure S 9: TGA analyses of Ru@IBOMC and used Ru@IBOMC

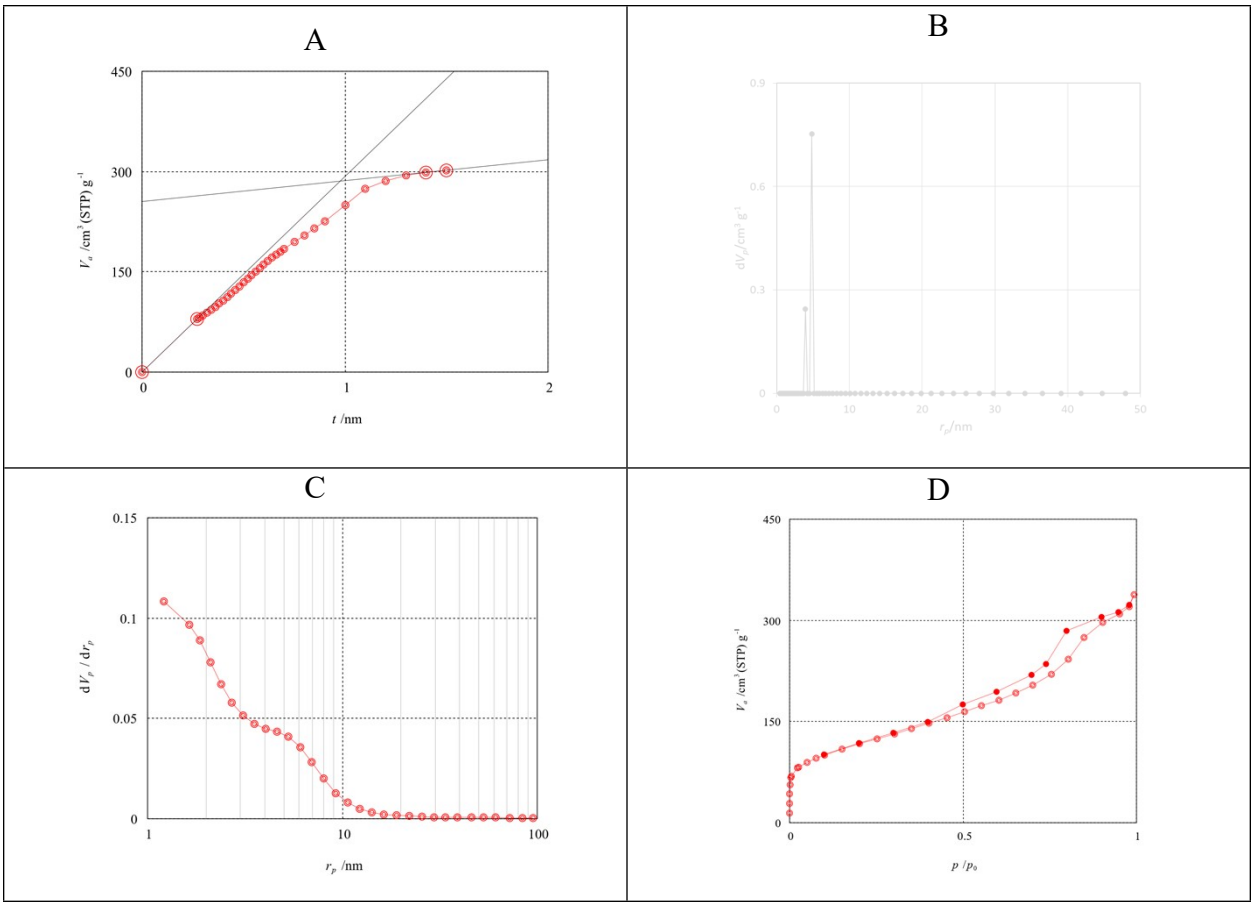

Figure S 10: A) t-plot of used-Ru@IBOMC, B) NLDFT of used-catalyst with PSD of $r_{p,peak}$ = 3.95 nm and 4.82 nm, C) BJH of used-catalyst, D) N_2 adsorption-desorption isotherms of used-catalyst.

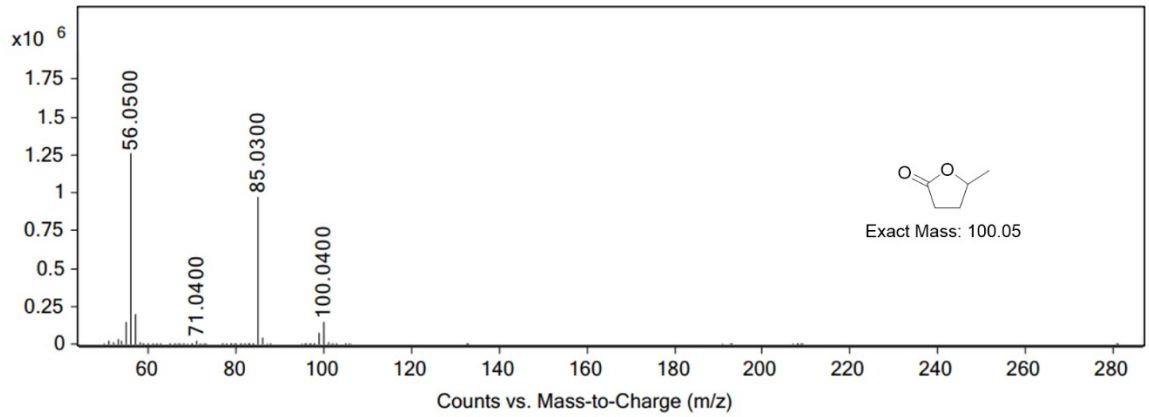

Peak List

m/z	z	Abund
51.03		22285.73
53.03		32432.7
55.05		148937.59
56.05		1256912.25
57.04		192936
71.04		23241.19
85.03	1	975626
86.03	1	46719.63
99.03		73991.97
100.04		142516.95

Figure S 11. Detection of GVL using GC Mass for conversion of LA into GVL, and reaction of LA with aniline at 90 °C

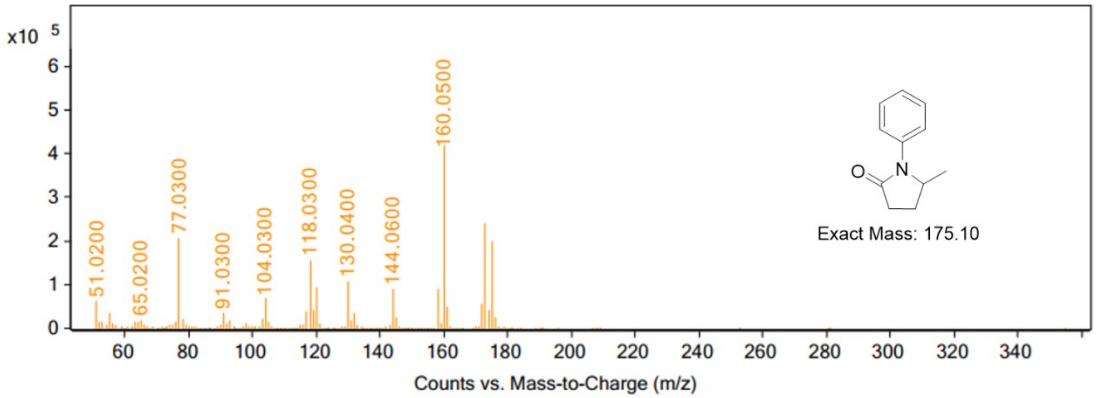

Peak List

m/z	z	Abund
77.03		207218.02
104.03		67859.24
118.03		154798.58
120.05	1	92667.89
130.04		106708.65
144.06		89353.63
158.04	1	90971.21
160.05	1	417323
173.05	1	239591.14
175.07	1	200247.94

Figure S 12. Detection of 5-methyl-1-phenylpyrrolidin-2-one using GC Mass in conversion of LA with aniline at 30 °C

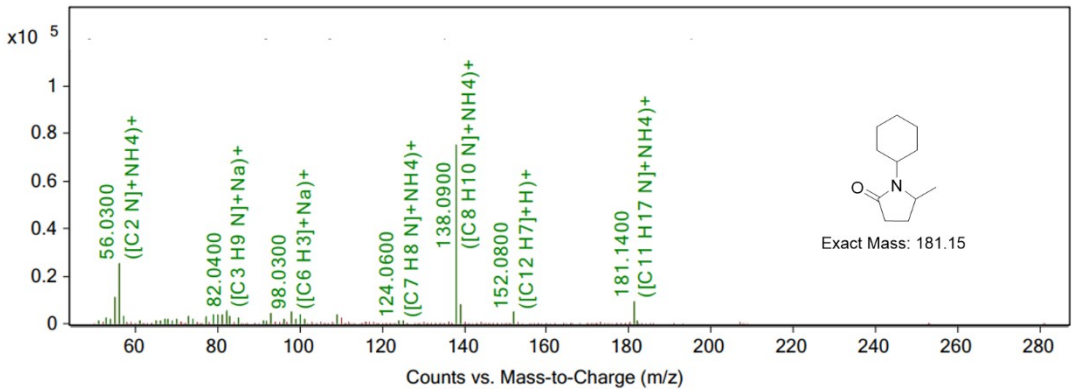

Peak List

m/z	z	Abund	Formula	Ion
55.03		11288.78	C3 H4 N	(M+H)+
56.03		25508.04	C2 N	(M+NH4)+
79.03		3976.64	C3 H6 N	(M+Na)+
82.04		5262.73	C3 H9 N	(M+Na)+
93.03		4513.85	C4 H8 N	(M+Na)+
98.03		4869.89	C6 H3	(M+Na)+
138.09	1	75176.09	C8 H10 N	(M+NH4)+
139.1	1	8072.8	C8 H10 N	(M+NH4)+
152.08	1	4838.54	C12 H7	(M+H)+
181.14	1	9447.82	C11 H17 N	(M+NH4)+

Figure S 13. Detection of aromatic lactam using GC Mass in conversion of LA with aniline at 90 °C

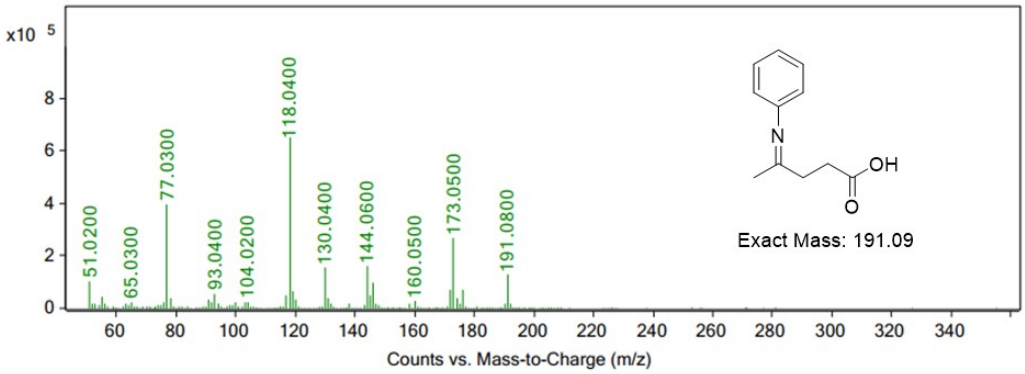

Peak List

m/z	z	Abund
51.02		104100.23
77.03	1	396827.06
118.04	1	648458.56
130.04		153150.03
144.06		157864.78
146.07	1	96662.36
172.06		69263.36
173.05	1	264020.84
176.04	1	70454.14
191.08	1	127390.34

Figure S 14. Detection of 4-(phenylimino)pentanoic acid using GC Mass in conversion of LA with aniline at 30 °C

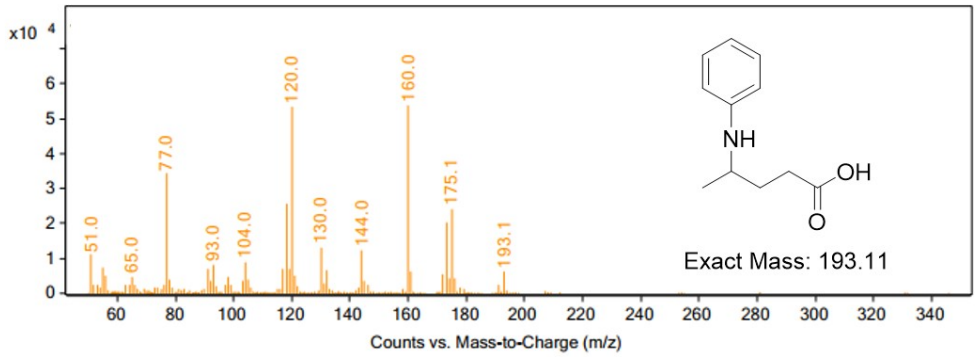

Peak List

m/z	z	Abund
51		11048.57
77		34167.51
104		8962.58
118		25567.66
120	1	53394.83
130		13109.53
144		12290.12
160	1	53913.11
173	1	20402.5
175.1	1	24173.49

Figure S 15. Detection of 4-(phenylamino)pentanoic acid using GC Mass in conversion of LA with aniline at 30 °C

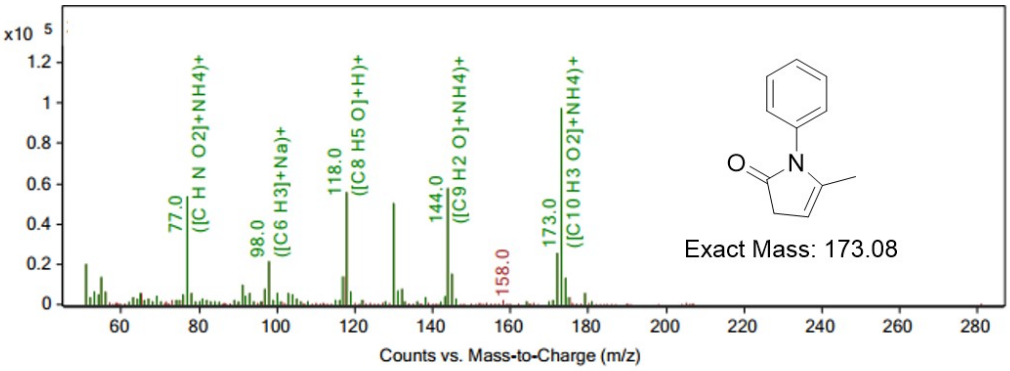

Peak List

m/z	z	Abund	Formula	Ion
51		20124.43	H O2	(M+NH4)+
77		53546.13	C H N O2	(M+NH4)+
98	1	21301.13	C6 H3	(M+Na)+
117		13965.25	C7 H N	(M+NH4)+
118	1	55263	C8 H5 O	(M+H)+
130	1	49939.3	C8 O	(M+NH4)+
144		57842.26	C9 H2 O	(M+NH4)+
145	1	15005.73	C10 H2	(M+Na)+
172		25528.98	C10 H5 N O2	(M+H)+
173	1	97076.36	C10 H3 O2	(M+NH4)+

Figure S 16. Detection of 5-methyl-1-phenyl-1,3-dihydro-2H-pyrrol-2-one using GC Mass in conversion of LA with aniline at 30 °C

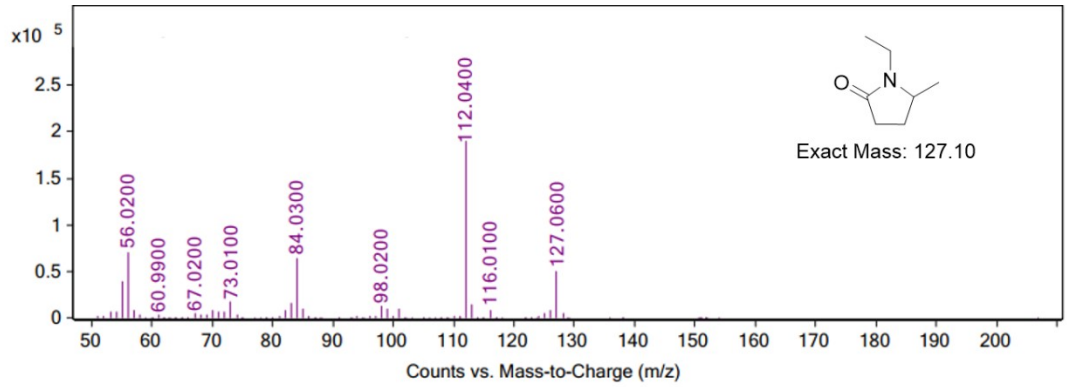

Peak List

m/z	z	Abund
55.01		39151.32
56.02		70848.02
73.01		17052.99
83.02		15572.32
84.03		64416.23
85.03		9670.85
98.02		11917.05
112.04	1	189529.08
113.03	1	13654.58
127.06	1	50151.69

Figure S 17. Detection of 1-ethyl-5-methylpyrrolidin-2-one with GC Mass in conversion of LA with acetonitrile

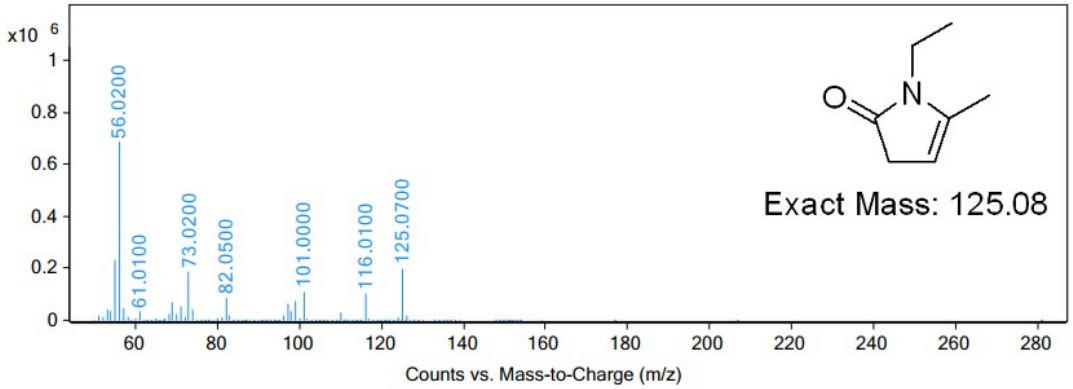

Peak List

m/z	z	Abund
55.01		228394.75
56.02	1	684832.56
69.05		70633.33
73.02		187378.84
82.05		84803.27
97.07		63746.45
99.02		75082.64
101		107219.32
116.01		102316.42
125.07	1	199170.88

Figure S 18. Detection of 1-ethyl-5-methyl-1,3-dihydro-2H-pyrrol-2-one with GC Mass in conversion of LA with acetonitrile

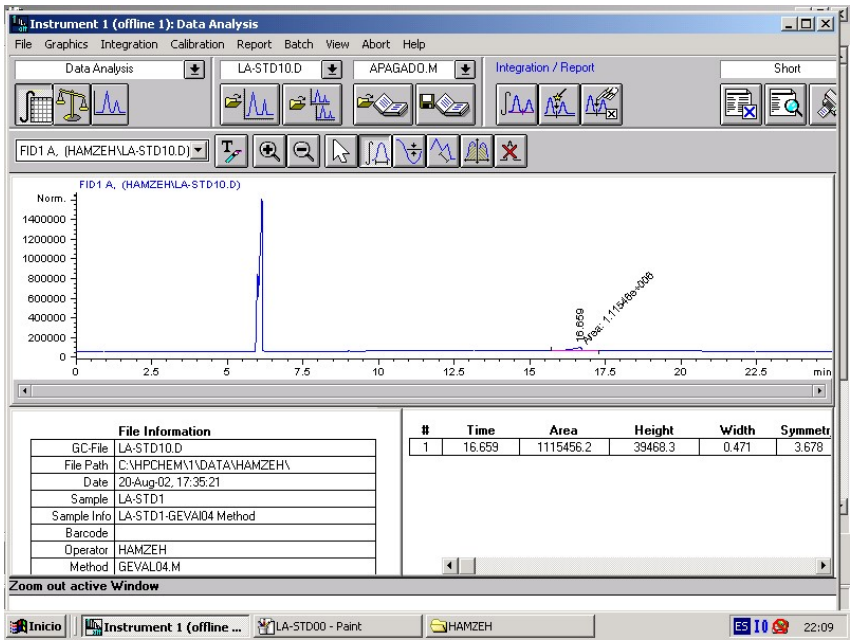

Figure S 19: Chromatogram of standard Levulinic acid in GC-FID

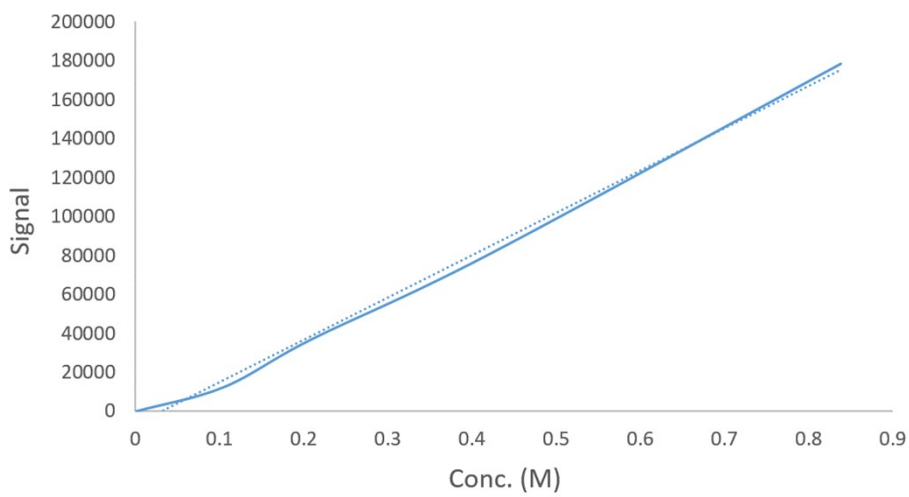

Figure S 20: GVL Calibration curve using GC-FID

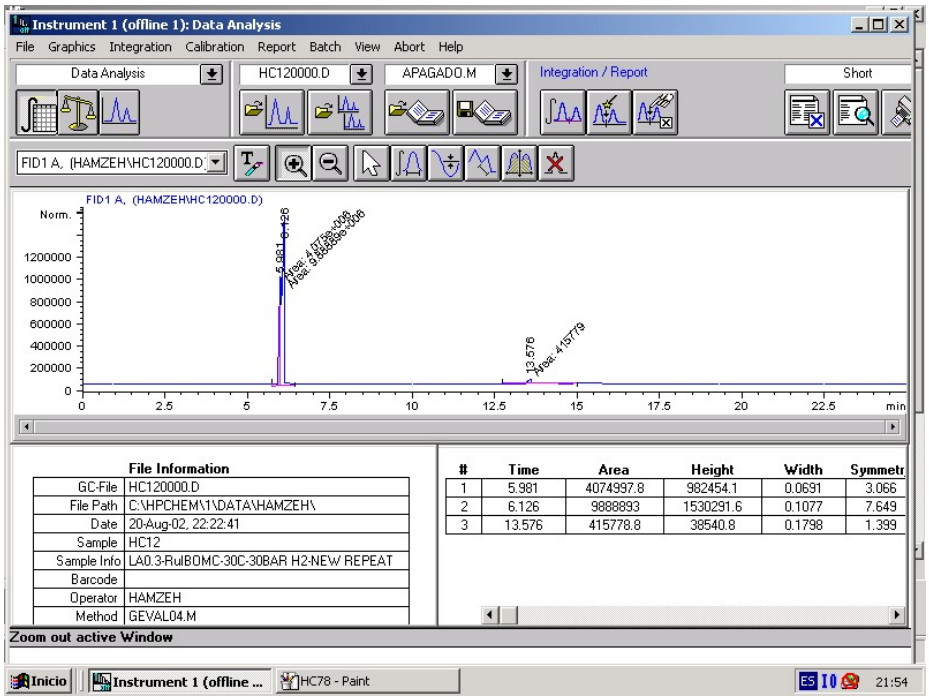

Figure S 21: Chromatogram of mixture of reaction after hydrogenation of Levulinic acid at room temperature in GC-FID

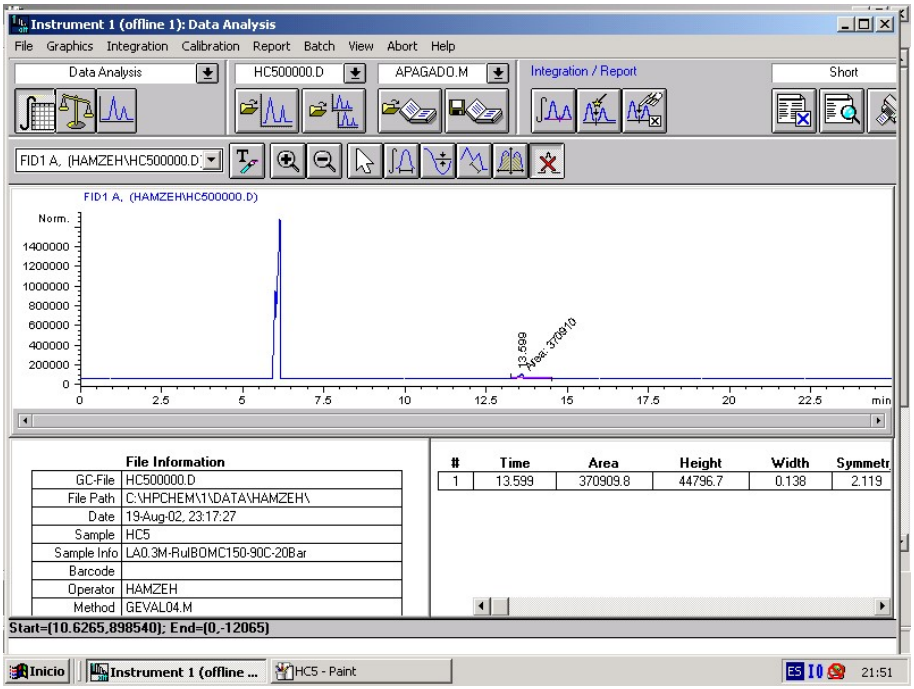

Figure S 22: Chromatogram of mixture of reaction after hydrogenation of Levulinic acid at 90 °C in GC-FID

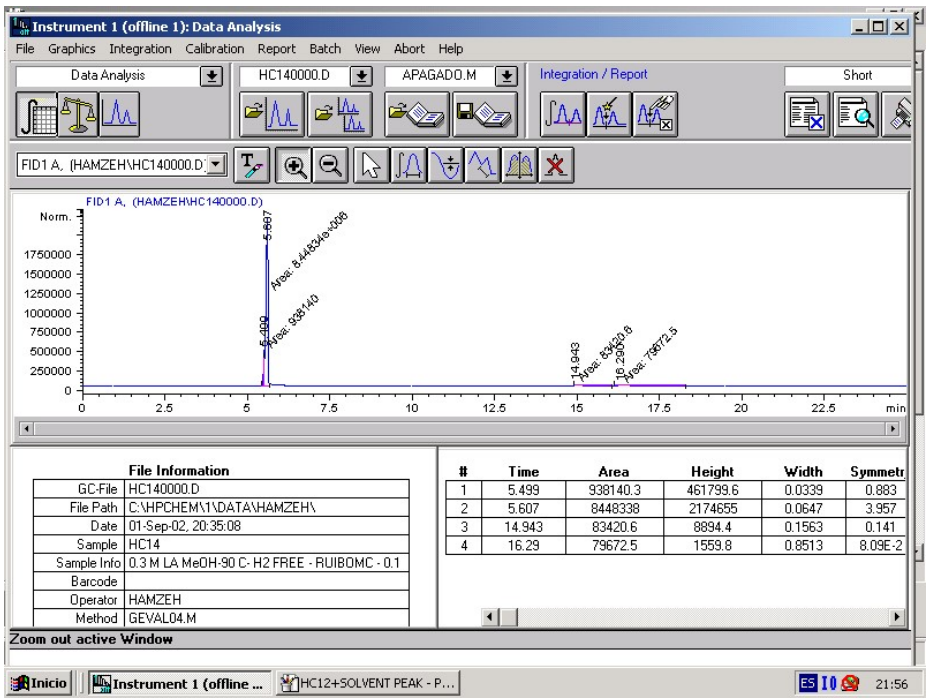

Figure S 23: Chromatogram of mixture of reaction after hydrogenation of Levulinic acid at H_2-free conditions in GC-FID

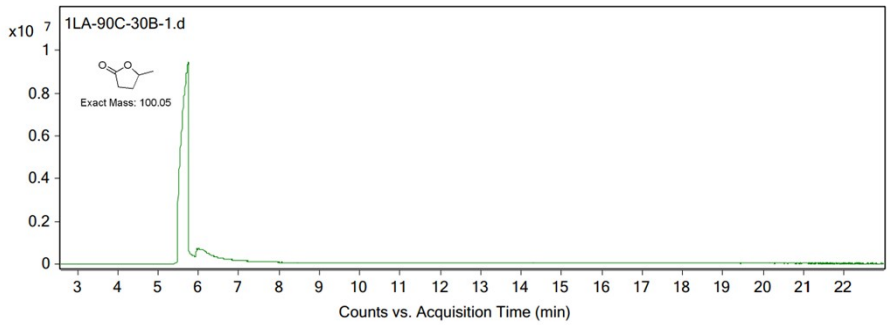

Integration Peak List

Peak	Start	RT	End	Height	Area	Area %
1	5.403	5.746	5.82	3690145.92	46431683.98	100
2	5.918	5.969	5.98	218107.63	607166.87	1.31

Figure S 24: Chromatogram of mixture of reaction after hydrogenation of Levulinic acid in GC-MS

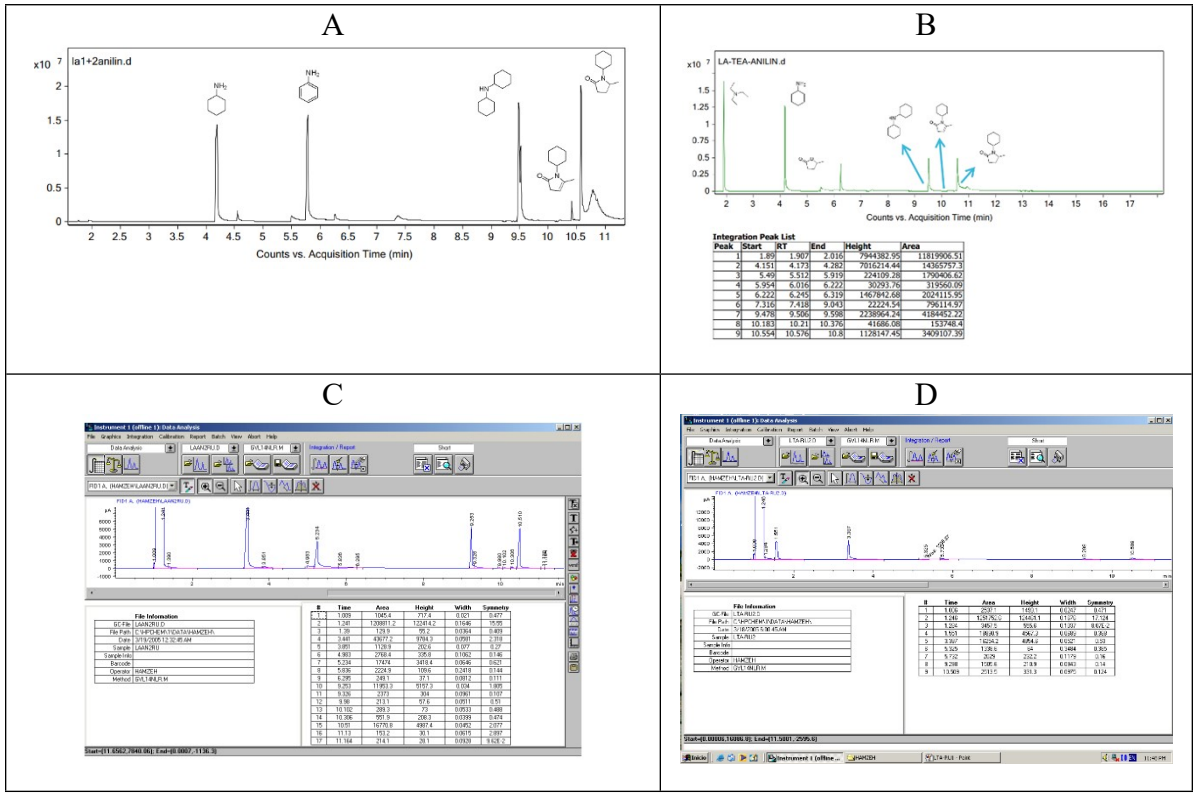

Figure S 25: A) Chromatogram of mixture of reaction after hydrogenation of Levulinic acid in the presence of Aniline at 90 °C using GC-MS; B) Chromatogram of mixture of reaction after hydrogenation of Levulinic acid 90 °C in the presence of Aniline and triethylamine as STD in GC-MS; C) Chromatogram of mixture of reaction after hydrogenation of Levulinic acid in the presence of Aniline using GC-FID; D) Chromatogram of mixture of reaction after hydrogenation of Levulinic acid in the presence of Aniline and TEA as STD using GC-FID.

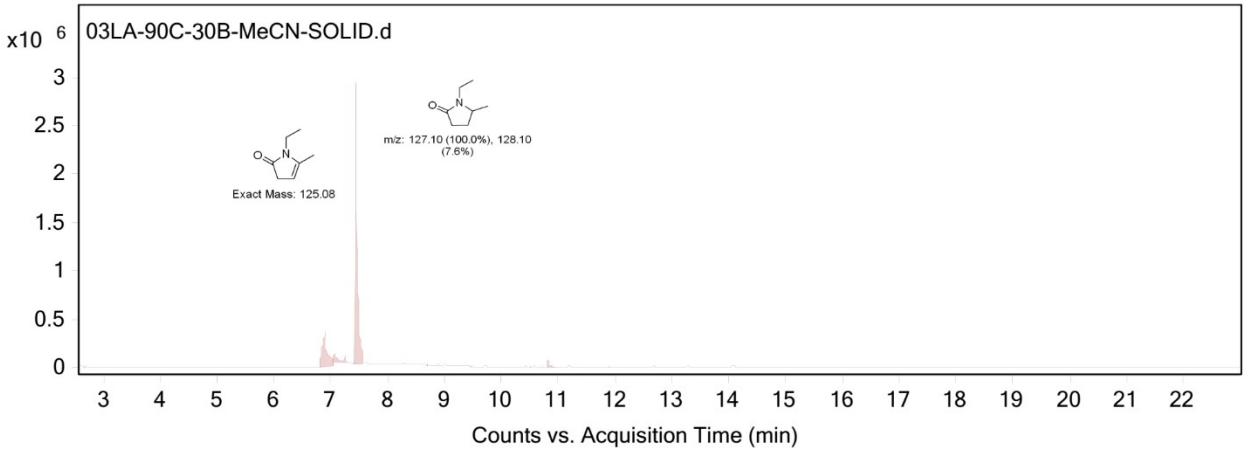

Integration Peak List

Peak	Start	RT	End	Height	Area
1	6.795	6.896	7.045	359950.82	2191504.26
2	7.045	7.062	7.222	80862.4	349890.3
3	7.222	7.245	7.342	68724.54	115657.72
4	7.411	7.434	7.548	2901664.3	6582517.11
5	10.793	10.815	10.959	75048.04	182562.57

Figure S 26: Chromatogram of mixture of reaction after hydrogenation of Levulinic acid in the presence of MeCN using GC-MS

References

[1] F. Kleitz, S. H. Choi, R. Ryoo, *Chemical Communications* **2003**, 2136-2137.
[2] H. H. Veisi, M. Akbari, B. Karimi, H. Vali, R. Luque, *Green Chemistry* **2023.** https://doi.org/10.1039/D3GC00117B